[Cu(m-MeCO2)2(4-Bzpy)]2 (4-Bzpy ¼ 4-benzylpyridine): Study of the intermolecular CeH/O hydrogen bonds at two temperatures

Joan Soldevila-Sanmartín [a], Marta Sanchez-Sala [a], Teresa Calvet [b], Mercè Font-Bardia [c], José A. Ayllón [a, **], Josefina Pons [a, *]

a Departament de Química, Universitat Aut onoma de Barcelona, 08193, Bellaterra, Barcelona, Spain
b Cristal·lografia, Mineralogia i Dip osits Minerals, Universitat de Barcelona, Martí i Franquès s/n, 08028, Barcelona, Spain
c Unitat de Difracció de Raig-X, Centres Científics i Tecnològics de la Universitat de Barcelona (CCiTUB), Universitat de Barcelona, Solé i Sabarís, 1-3, 08028, Barcelona, Spain

Josefina.Pons@uab.es, (J. Pons)..

joseantonio.ayllon@uab.es

ABSTRACT:

Cu(m-MeCO2)2(4-Bzpy)]2 (4-Bzpy ¼ 4-benzylpyridine) has been synthesized by reaction of [Cu(m-MeCO2)2(H2O)]2 with 4-Bzpy in methanol at room temperature. The compound was characterized by Elemental Analysis, ATR-FTIR and X-ray Powder Diffraction. The molecular structure was determined by single crystal X-ray diffraction analysis at 100 K and 303 K. The compound consists of binuclear units where both Cu(II) atoms are linked by four syn-syn carboxylate bridges, showing a paddle-wheel unit. The role of CeH/O hydrogen bonds in the establishment of its supramolecular network is discussed, comparing the resulting structural parameters at the two different temperatures. Finally, the thermal variation of XpT for compound 1 has also been studied, suggesting an antiferromagnetic Cu/Cu interaction (J¼ 311 cm 1), which agrees with the presence of four m-kO-kO0 carboxylates bridging the metallic centers in the binuclear complex.

1. INTRODUCTION

The synthesis, crystal structure and properties of numerous copper(II) carboxylates have already been extensively studied, garnering great interest due to their diverse structural features [1e4], spectroscopic, magnetic and catalytic activities [5,6]. Furthermore, a large number of paddle-wheel type binuclear copper(II) carboxylate adducts [Cu(m-RCO2)2(L)]2, where L is an apical ligand with oxygen or nitrogen atom, have been reported in the literature, many of them featuring pyridine groups [7e12]. In their synthesis, metal carboxylates, along with N- and O- donor atoms, have often been used with the aim of constructing paddle-wheels with mixed ligands, which might have interesting structural features with useful applications.

Binuclear paddle-wheel Cu(II) units have attracted attention as building-blocks for Supramolecular Metal Organic Frameworks (SMOFs), porous materials sustained by intermolecular weak forces [13,14]. SMOFs have attracted great attention due the possibility of out-performing Metal Organic Frameworks (MOFs) in its industrial applications due to enhanced host-guest interactions and wetprocessability. Among the weak forces that hold SMOFs together, hydrogen bonds have a special importance as they are among the strongest intermolecular forces, and play a central role in crystal engineering [15,16]. Beyond the classical XeH$$$O bond (X ¼ N, O or halogen), nowadays the importance of CeH/O bonds is widely recognized, despite strong controversy over past years [17e20]. Although CeH/O bonds have been extensively studied regarding organic compounds, its importance in coordination chemistry is now being recognized [21e23].

As a continuing effort to enhance the comprehension of structure, reactivity and different properties of the copper(II) carboxylate compounds, we employed pyridine ligands with the potential to incorporate intra- and intermolecular interactions (e.g. hydrogen bond, p-p stacking, etc) [1,2]. In this context, we have studied the synthesis and structural characterization of 1,3-benzodioxole-5-carboxylic acid (HPip) and different amines (3-phenylpyridine and 4-phenylpyridine) with Zn(MeCO2)2$2H2O and Cd(Me-CO2)2$2H2O obtaining the compounds [Zn(m-Pip)2(3-Phpy)]2, [Zn(m-Pip)2(4-Phpy)]2, [Cd(m-Pip)(Pip)(3-Phpy)2]2 and [Cd(m-Pip)(- Pip)(4-Phpy)2]2 coordination dimers [24]. We also studied the reaction of the same ligand (HPip) with [Cu(m-MeCO2)2(H2O)]2 and pyridine ligands (dPy ¼ 3-Phpy, 4-Bzpy and 4-Phpy) obtaining [Cu(Pip)2(3-Phpy)(H2O)] and [Cu(Pip)2(4-Bzpy)2][Cu(Pip)2(4-Bzpy)2(HPip)] monomeric compounds and [Cu(m-Pip)2(dPy)]2 (dPy ¼ 3-Phpy, 4-Bzpy) and [Cu(m-Pip)(Pip)(4-Phpy)2]2 dimeric compounds [25]. Moreover, when the reaction of HPip and [Cu(m-MeCO2)2(H2O)]2 in 1:1 M:L is assayed, heteroleptic compound is obtained [Cu(m-Pip)(m-MeCO2)(MeOH)]2 [26].

Recently in our group, we have assayed the reaction of [Cu(m- MeCO2)2(H2O)]2 and pyridine ligands (dPy ¼ 3-Phpy, 2-Bzpy and 4- Acpy) obtaining always paddle-wheel compounds [Cu(m-MeCO2)2(dPy)]2 [27]. As a continuation of this work, in this manuscript we are interested in the reaction of [Cu(m- MeCO2)2(H2O)]2 with 4-Bzpy. In particular, we report the synthesis, IR

spectroscopy and X-ray crystal structure of the resulting compound [Cu(MeCO2)2(4-Bzpy)]2 (1). Furthermore, the X-ray crystal structurewas determined at two different temperatures,100 K (1A) and 303 K (1B), which allowto study the effect of temperature in its supramolecular structure, with special focus on the role of CeH/O hydrogen bonds. Finally, magnetic studies for this compound were also carried out.

2. RESULTS AND DISCUSSION

2.1. Synthesis and general characterization

Complex 1, was prepared in MeOH at room temperature via combination of [Cu(m-MeCO2)2(H2O)]2 and 4-benzylpyridine (4- Bzpy), yielding complex [Cu(m-MeCO2)2(4-Bzpy)]2, a paddlewheel product. In this reaction, the coordinated apical H2O molecules were displaced by the pyridine-derived ligand. The corresponding crystals suitable for X-ray crystallographic analysis were grown via slow evaporation of their mother liquors. The obtained compound is green and elemental analyses agree with the proposed formula. Phase purity of the compound was confirmed via a whole pattern matching process. The experimental powder X-ray diffraction (PXRD) is compared against a pattern calculated using DAjust software [28], which considers the defining parameters (space group, symmetry group, unit cell parameters ….) of the solved crystal structure. The result is graphically represented using WinPlotR software [29] (SI, Fig. S1).

Shifts in the ATR-FTIR spectrum of the compound compared to the reagents, [Cu(m-MeCO2)2(H2O)]2 and 4-Bzpy (SI, Fig. S2-S4), confirms their coordination to the metal centre. Bands assignable to carboxylate group give key information about the coordination mode. This compound displays the bands attributable to carboxylate anion at 1600 cm 1 for nas(COO) and 1423 cm 1 for ns(COO), the difference between nas(COO) and ns(COO) is 177 cm 1, indicating bidentate bridging coordination mode of the acetate group [30,31]. The bands attributable to the aromatic groups n(C] C)ar, n(C]N)ar, d(CeH)ip and d(CeH)oop are also observed [32]. The IR spectral data thus clearly lend support to the structure determined by the X-ray diffraction method (SI, Fig. S4).

2.2. Crystal structure of [Cu(m-MeCO2)2(4-Bzpy)]2 (1)

The compound was isolated as green prism-like crystals. Single crystal X-ray diffraction revealed that the compound is [Cu(m- MeCO2)2(4-Bzpy)]2 (1) and crystallizes in the monoclinic space group P21/c. The representation is shown in Fig. 1. Selected bond distances and angles are provided in Table 1. The Cu atoms adopt the [CuO4N] coordination mode, with four oxygen atoms from different carboxylates and one nitrogen atom from 4-Bzpy ligand. The structure consists in a centrosymmetric binuclear copper(II) unit and is typical of binuclear [M2(carboxylate) 4L2] complexes [33]. The carboxylate groups of the acetate ligands display a paddle-wheel-like arrangement, with four bridging acetate ligands in a syn-syn coordination mode. At 100 K, the Cu$$$$Cu separation is 2.6222 (6) Å, whereas at 303 K is 2.6311 (10). Both values are comparable to those reported for paddlewheel complexes with similar structure [25,26,34,35]. The tetra- carboxylate bridging framework accommodates a metal-metal separation up to 3.452 Å [33]. Each Cu(II) has a slightly distorted square-

pyramidal coordination geometry (t ¼ 1.33 10 3 at 100 K, 5.17 10 3 at 303 K) [36], with the apex provided by axial coordination of the 4-Bzpy ligand. The CueO bond distances range from 1.963 (4) to 1.975 (4) Å and the Cu(1)eN(1) bond length is 2.1828 (19) Å at 100 K and 2.191 (4) at 303 K, which are comparable with the reported values in [Cu2(m-MeCO2)2(L)]2 (L ¼ 4-dimethylaminopyridine [37], nicotinamide [38], N-2- acetamidopyridine [39], 2-[N-(2-pyridyl)carbomoylpyridine [38], and 4-pyridylmethanol [40].

Intramolecular distances are barely affected by the change in temperature, as the differences between both temperatures are in the range of 0.002 Å to 0.01 Å. These values are almost on the order of magnitude corresponding to the standard deviation of the bond lengths in the elucidated crystal structure, thus being negligible. The effect on intramolecular angles is more noticeable, as the differences range between 0.40 and 3.57 , being especially noticeable the effect on the O3eCu1eN1 (increase in 3.57) and O4#1-Cu1-N1 (decrease in 3.17) angles. Those slight changes in the bond angles result in a slight increase in t:1.33 10 3 at 100 K, 5.17 10 3 at 303 K, however, the overall coordination geometry of the Cu(II) cation remains unchanged (Table 1).

2.3. Extended structures of 1 (A and B)

The supramolecular structure of 1 is completely dominated by non-covalent CeH/O interactions at both temperatures (100 K and 303 K). June Sutor, pioneer researcher on the structural role of CeH/O bonds established its limits based on a d (H/O) distance [41,42] inferior to the sum of the Van der Waals radii of H and O (2.72 Å according to Bondi [43] or 2.61 Å according to Rowland and Taylor [44]). On the other hand, studies carried out by Steiner show that most of CeH/O bonds are comprised in the range of d (H/O) < 2.7 Å [45], which is more or less coincident with the sum of Van der Waals radii of H and O. However, this same Steiner [45] affirms that using either the d (H/O) distance or the sum of Van derWaals radii as a limit is an arbitrary election and could result in dismissing important interactions, and demonstrates that CeH/O interactions can be found up to d (H/O) distances of 3.20 Å [15,17,20]. In this work, d (H/O) interactions up to 2.90 Å will be considered, for the purposes of comparing the structural parameters of compound 1 at 100 K and 303 K.

At low temperature (100 K) (1A) the main CeH/O hydrogen bonds results in a three-dimensional expansion (Fig. 2). They are formed by the interaction of coordinated oxygens of the acetate moiety with methyl and pyridyl functional groups from the acetate and pyridine ligands. The strongest, responsible for the expansion in the c direction is C16eH16C/O3, O3 belonging to the coordinated acetate and H16C to the methyl group of neighbouring acetate. This interaction results in the formation of a 1D chain (Fig. 3, top). The second one, responsible for the expansion in both b and c direction, involves O4 of the same coordinate acetate and H2, a hydrogen in meta position of a neighbouring pyridyl ring resulting in the formation of 2D layers in the bc plane (Fig. 3, down). Other minor interactions strengthen the plane,

such as C14eH14C/O3, which connects the same O3 that participates in the first mentioned intermolecular interaction with another methyl group. Those three interactions are within the range of d (H/O) < 2.7 Å and can be he considered the main ones in this structure. The final 3D expansion is caused by the interaction between O4 and H10 (Fig. 3, top) a hydrogen of the benzene ring of 4-Bzpy, which holds the layer together albeit this interaction is much weaker when compared to the previous ones as d (H/O) > 2.7 Å (Table 2).

When the structure is measured at higher temperatures (303 K) (1B), the first thing we should note is that the expansion of the cell is very small, representing only an increase in 3% in volume. At this temperature, only one hydrogen bond with d (H/O) < 2.7 Å is present, this interaction is C2eH2/O4. Therefore, due its propagation in both b and c directions, it is confirmed that the supramolecular 2D layers are conserved. The rest of the interactions (O3/H16C, O3/H14C and O4/H10) are weakened at this temperature because d (H/O) distance increases by 0.091 Åe0.103 Å, resulting in d (H/O) > 2.7 Å (Fig. 4). These results agree with similar values obtained in previous studies reported in the literature [45,46]. The fact that these interactions are weakened at higher temperatures suggests relatively weak interaction strength.

2.4. Magnetic properties of compound 1

For compound 1, the cpT values reach a maximum at around 300 K and decreases upon cooling until around 65 K, where the formation of a plateau-like region can be foreshadowed, as seen in Fig. 5. This behaviour suggests a strong antiferromagnetic Cu$$$$Cu interaction, which is typical of Cu(II) paddle-wheels [26]. The magnetic behaviour of this compound can be modelled according to the classical Bleany and Bowers S ¼ 1/2 dimer model [47]. This model reproduces accurately the magnetic properties on the selected temperature range. Found parameters are: g ¼ 2.00; J (cm 1)¼ 311; r (%) ¼ 2.39; H ¼ -JSiSiþ1. These values are in agreement with other reported values in the literature, including the original Cu(II) acetate complex (J¼ 284 cm 1) [48].

3. CONCLUSIONS

We described [Cu(m-MeCO2)2(4-Bzpy)]2 (1) formed by [Cu(m-MeCO2)2]2 paddle-wheel units and 4-benzylpyridine coordinated to the apical positions of copper atoms. The compound has been fully characterized to investigate their structural and spectroscopic properties. Moreover, a study of its supramolecular structure is carried out at 100 K (1A) and 303 K (1B) to observe the effect of temperature on its structural parameters. Single crystal X-ray diffraction shows that the main forces involved in sustaining the supramolecular 2D layers are CeH/O bonds. The unit cell of 1 undergoes a minor expansion (approx. 3% in volume) when the temperature is changed between 100 K and 303 K, and the effects of this temperature increase on the atomic bonds are barely noticeable. The intermolecular structure is retained as seen via PXRD. The CeH/O are weakened when the temperature is increased, as d (H/O) increases 0.096 Å on average for the selected interactions, which is in range of previously reported studies [45]. This results in having three interactions with d (H/O) < 2.7 Å at 100 K and only one interaction with d (H/O) < 2.7 Å at 303 K. The dimeric complex shows a strong intradimer Cu/Cu antiferromagnetic interaction, which is in agreement with the values of similar compounds reported in the literature [26,48].

4. EXPERIMENTAL

4.1. Materials and general details

Cu(II) acetate monohydrate (Cu(m-MeCO2)2$H2O), 4-benzylpyridine (4-Bzpy) and methanol (MeOH) were purchased from Sigma-Aldrich and used without further purification. All reactions and manipulation were carried out in air. Elemental analyses (C, H, N) were carried out by the staff of Chemical Analysis Service of the Universitat Aut onoma de Barcelona on a Euro Vector 3100 instrument. IR spectra were recorded on a Tensor 27 (Bruker) spectrometer, equipped with an attenuated total reflectance (ATR) accessory model MKII Golden Gate with diamond window in the range 4000e600 cm 1. Powder X-ray diffraction patterns were measured with a Siemens 5000 apparatus using the CuKa radiation. Patterns were recorded from 2q ¼ 5 e50 with a step scan of 0.02 counting for 1s at each step. Data was processed with DAjust software [28] and graphically represented using WinPlotR software [29]. Magnetic measurements from 65 to 300 K were carried out with a Quantum Design MPMS-5S SQUID susceptometer using a 100 Oe field.

4.2. Synthesis of [Cu(m-MeCO2)2(4-Bzpy)]2 (1)

To a solution of 4-benzylpyridine (0.103 g, 0.610 mmol), in MeOH (20 mL), Cu((m-MeCO2)2H2O (0.109 g, 0.550 mmol) in MeOH (20 mL) was added. The resulting light blue solutionwas allowed to evaporate at room temperature. When the solution volume was reduced to 20 mL, a green crystalline solid appeared; it was filtered, washed with cold MeOH (5 mL) and dried in the air.

Yield: 572mg (81.4%) (respect to Cu((m-MeCO2)2H2O). Elemental Analyses: Calc. for C32H34N2O8Cu2 (701.69): C, 54.77; H, 4.88; N, 3.99. Found: C, 55.05; H, 4.93; N, 3.90%. ATR-FTIR (wavenumber, cm 1): 3062-3004(w) [n(CeH)ar], 2995-2924(w) [n(CeH)al],1600(s) [nas (COO), n(C]C)/n(C]N)], 1558(w), 1494(w), 1423(s) [ns (COO), d(C]C)/d(C]N)], 1351(w), 1220(m), 1095(m), 1069(w), 1051(w), 1033(w), 1016(m) [d(CeH)ip], 858(w), 831(w), 793 (m), 738(m), 681(s) [d(CeH)oop], 615(m).

The variation of the magnetization with temperature of 0.1356 g (0.1930 mmols) in a 100 Oe field was measured. The calculated diamagnetic contribution of this compound was found to be 1.85$10 4 cm3/mol using Pascal's constants [49].

4.3. X-ray crystallography

A green prism-like specimen was used for the X-ray crystallographic analysis. The X-ray intensity data were measured on a D8 Venture system equipped with a multilayer mono-chromate and a Mo microfocus (l ¼ 0.71073 Å). For this compound (100 K (1A), 303 K (1B)), the frames were integrated with the Bruker SAINT Software package using a narrow-frame algorithm. At 100 K (1A), the integration of the data using a monoclinic unit cell yielded a total of 16918 reflections to a maxim q

angle of 26.06 (0.81 Å resolution), of which 3013 were independent (average redundancy 5615, completeness ¼ 99.8%), Rint ¼ 5.81%, Rsig ¼ 3.78%) and 2518 (83.57%) were greater than 2s(F2). The calculated minimum and maximum transmission coefficients (based on crystal size) are 0.5924 and 0.7453. At 303 K (1B), the integration of the data using a monoclinic unit cell yielded a total of 20586 reflections to a maxim q angle of 26.40 (0.80 Å resolution), of which 3193 were independent (average redundancy 6447, completeness ¼ 99.2%), Rint ¼ 3.42%, Rsig ¼ 2.18%) and 2866 (89.76%) were greater than 2s(F2). The calculated minimum and maximum transmission coefficients (based on crystal size) are 0.6490 and 0.7454.

The structures were solved using the Bruker SHELXTL Software, package and refined using SHELX [50]. At 100 K (1A), the final anisotropic full-matrix least-squares refinement on F2 with 201 variables converged at R1 ¼3.24%, for the observed data and wR2 ¼ 8.12% for all data. At 303 K (1B) the final anisotropic fullmatrix least-squares refinement on F2 with 201 variables converged at R1 ¼5.17%, for the observed data and wR2 ¼16.93% for all data. For 1A and 1B, the final cell constants and volume, are based upon the refinement of the XYZ-centroids of reflections above 20 s(I). Data were corrected for absorption effects using the multi-scan method (SADABS). Crystal data and relevant details of structure refinement for compound 1 (1A, 1B), are reported in Table 3. Complete information about the crystal structure and molecular geometry is available in CIF format as Supporting Information. CCDC 1585996 (1A), and 1585997 (1B) contain the supplementary data for this paper. Molecular graphics were generated with the program Mercury 3.6 [51,52]. Color codes for all molecular graphics: blue (Cu), light blue (N), red (O), grey (C), white (H).

ACKNOWLEDGEMENTS

This workwas financed by the Spanish National Plan of Research MAT2015-65756-R and by 2014SGR260 and 2014SGR377 projects from the Generalitat de Catalunya. J.S. also acknowledges the Universitat Autònoma de Barcelona for his pre-doctoral grant.

APPENDIX A. SUPPLEMENTARY DATA

Supplementary data related to this article can be found at https://doi.org/10.1016/j.molstruc.2018.06.056.

REFERENCES

[1] C.-S. Liu, J.-J. Wang, L.-F. Yan, Z. Chang, X.-H. Bu, E.C. Se~nudo, J. Ribas, Inorg. Chem. 46 (2007) 6299e6310.

[2] B. Moulton, M.J. Zaworotko, Chem. Rev. 101 (2001) 1629e1658.

[3] A.J. Blake, N.R. Champness, P. Hubberstey, W.-S.- Li, M.A. Withersby, M. Schr€oder, Coord. Chem. Rev. 183 (1999) 117e138.

[4] M. Kato, Y. Muto, Coord. Chem. Rev. 92 (1988) 45e83.

[5] J. Moncol, M. Mudra, P. L onnecke, M. Hewitt, M. Valko, H. Morris, J. Svorec, M. Melnik, M. Mazur, M. Koman, Inorg. Chim. Acta 360 (2007) 3213e3225.

[6] G.C. Campbell, J.F. Haw, Inorg. Chem. 27 (1988) 3706e3709.

[7] N. Abdullah, Y. Al-Hakem, N. Abdullah, H. Samsudin, N.S.A. Tajidi, Asian J. Chem. 26 (2014) 987e990.

[8] R. Sarma, J.B. Baruah, J. Coord. Chem. 61 (2008) 3329e3335.

[9] R. Cejuto, G. Alzuet, J. Borr as, M. Liu-Gonzalez, F. Sanz-Ruiz, Polyhedron 21 (2002) 1057e1061.

[10] F.P.W. Agterberg, H.A.J. Prov o Kluit, W.L. Driessen, H. Oevering, W. Buijs, M.T. Lakin, A.L. Spek, J. Reedjick, Inorg. Chem. 36 (1997) 4321e4328.

[11] A. Ozarowski, C. Calzado, R.P. Sharma, S. Kumar, J. Jezierska, C. Angeli, F. Spizzo, V. Ferretti, Inorg. Chem. 54 (2015) 11916e11934.

[12] R.P. Sharma, A. Saini, P. Venugopalan, J. Jezierska, V. Ferretti, Inorg. Chem. Commun. 20 (2012) 209e213.

[13] G. Beobide, O. Castillo, J. Cepeda, A. Luque, S. P erez-Y a~nez, P. Roman, J. Thomas-Gipson, Coord. Chem. Rev. 257 (2013) 2716e2736.

[14] G. Beobide, O. Castillo, A. Luque, S. P erez-Y a~nez, CrystEngComm 17 (2015) 051e3059.

[15] G.R. Desiraju, Acc. Chem. Res. 35 (2002) 565e573.

[16] Y.-F. Han, Y.-X. Yuan, H.-B. Wang, Molecules 22 (2017) 266e300.

[17] T. Steiner, Angew. Chem. Int. Ed. 41 (2002) 48e76.

[18] S. Scheiner, J. Phys. Chem. B 109 (2005) 16132e16141.

[19] S. Scheiner, Phys. Chem. Chem. Phys. 13 (2011) 13860e13872.

[20] C.H. Schwalbe, Crystallogr. Rev. 18 (2012) 191e206.

[21] M. Enamullah, M.A. Qudus, M.A. Halim, M.K. Islam, V. Vasylyeva, C. Jainak, Inorg. Chim. Acta 427 (2015) 103e111.

[22] T. Yao, J. Lu, D. Li, J. Dou, Acta Cryst. C70 (2014) 364e367.

[23] K.A. Sidiqqui, J. Mol. Struct. 65 (2012) 4168e4176.

[24] M. Guerrero, S. V azquez, J.A. Ayll on, T. Calvet, M. Font-Bardía, J. Pons, ChemistrySelect 2 (2017) 632e639.

[25] J. Soldevila-Sanmartín, J.A. Ayll on, T. Calvet, M. Font-Bardía, J. Pons, Polyhedron 126 (2017) 184e194.

[26] J. Soldevila-Sanmartín, J.A. Ayll on, T. Calvet, M. Font-Bardía, C. Domingo, J. Pons, Inorg. Chem. Commun. 71 (2016) 90e93.

[27] M. Guerrero, J.A. Ayll on, T. Calvet, M. Font-Bardia, J. Pons, Polyhedron 134 (2017) 107e113.

[28] O. Vallcorba, J. Rius, C. Frontera, I. Peral, C.J. Miravitlles, J. Appl. Cryst. 45 (2012) 844e848.

[29] T. Roisnel, I. Rodríguez-Carvajal, Mater. Sci. Forum 378e381 (2001) 118e123.

[30] K. Nakamoto, Infrared and Raman Spectra of Inorganic and Coordination Compounds, in: Applications in Coordination, Organometallic and Bioinorganic Chemistry, sixth ed., Wiley Interscience, New York, USA, 2009.

[31] G.B. Deacon, R.J. Phillips, Coord. Chem. Rev. 88 (1980) 227e250.

[32] D.H. Williams, I. Fleming, Spectroscopic Methods in Organic Chemistry, McGrawHill, London, UK, 1995.

[33] T. Allman, R.C. Goel, N.K. Jha, A.L. Beauchamp, Inorg. Chem. 23 (1984) 914e918.

[34] R.C. Santra, K. Sengupta, R. Dey, T. Shireen, P. Das, P.S. Guin, K. Mukhopadhyay, S. Das, J. Coord. Chem. 67 (2014) 265e285.

[35] A.V. Yakovenko, S.V. Kolotilov, O. Cador, S. Golhen, L. Ouahab, V.V. Pavlishchuck, Eur. J. Inorg. Chem. (2009) 2354e2361.

[36] W. Addison, T.N. Rao, J. Chem. Soc. Dalton Trans. (1984) 1349e1356.

[37] X-Jun Feng, H-Ze Dong, W. Huang, Acta Cryst. E63 (2007) m1105em1106.

[38] B. Kozlevcar, I. Leban, I. Turel, P. Segedin, M. Petric, F. Pohleven, A.J.P. White, D.J. Williams, J. Sieler, Polyhedron 18 (1999) 755e762.

[39] M.A. Pauly, E.M. Erwin, D.R. Powell, G.T. Rowe, L. Yang, Polyhedron 102 (2015) 722e734.

[40] N.N. Hoang, F. Valach, M. Melnik, Acta Cryst. C49 (1993) 467e469.

[41] D.J. Sutor, Nature 195 (1962) 68e69.

[42] D.J. Sutor, J. Chem. Soc. (1963) 1105e1110.

[43] A. Bondi, J. Phys. Chem. 68 (1964) 441e451.

[44] R.S. Rowland, R. Taylor, J. Phys. Chem. 100 (1996) 7384e7391.

[45] T. Steiner, W. Saenger, J. Am. Chem. Soc. 114 (1992) 10146e10154.

[46] D. Ishii, T. Yamada, T. Iyoda, H. Yoshida, M. Nagagawa, Chem. Lett. 35 (2006) 1394e1395.

[47] B. Bleaney, K.D. Bowers, Proc. R. Soc. Lond. Ser. A. 214 (1952) 451e465.

[48] M. Melnik, Coord. Chem. Rev. 42 (1982) 259e293.

[49] G.A. Bain, J.F. Berry, J. Chem. Educ. 85 (2008) 532e536.

[50] G.M. Sheldrick, Acta Cryst. C71 (2015) 3e8.

[51] C.F. Macrae, P.R. Edgington, P. McCabe, E. Pidcock, G. Shields, R. Taylor, M. Towler, J. van de Streek, J. Appl. Crystallogr. 39 (2006) 453e457.

[52] C.F. Macrae, I.J. Bruno, J.A. Chisholm, P.R. Edgington, P. McCabe, E. Pidcock, I. Rodriguez-Monge, R. Taylor, J. van de Streek, P.A. Wood, J. Appl. Crystallogr. 41 (2008) 466e470.

Legends to figures

Figure. 1 [Cu(m-MeCO2)2 (4-Bzpy)]2 at 100 K (1A) showing the labelling scheme for relevant atoms. See Table 1 for selected values of bond lengths and bond angles.

Figure.2 3D network generated by propagating intermolecular contacts determined at 100 K. View along the a axis (top). View along the c axis (down). All hydrogen atoms are omitted for clarity, except those participating in hydrogen bonds.

Figure.3. Detail of the propagation of the C16eH16C/O3 and C10eH10/O4 hydrogen bonds (blue lines). Note the 1D chains parallel to the c axis (100 K) generated by C16eH16/O3 and the expansion along the a direction generated by the C10eH10/O4 interaction (top). Detail of the propagation of the C14eH14C/O3 and C2eH2/O4 hydrogen bonds (blue lines, down). Note the 2D layers parallel to the bc plane (100 K). All hydrogen atoms are omitted for clarity, except those participating in hydrogen bonds. (For interpretation of the references to colour in this figure legend, the reader is referred to the Web version of this article.)

Figure.4 Comparative diagram showing the extend of the H-bond (blue lines) network at 100 K and 303K. View along the a axis (top). View along the c axis (down). Note that although the 2D layers parallel to bc plane are still held together, but how the interaction along the a axis disappears (down). All hydrogen atoms are omitted for clarity, except those participating in hydrogen bonds. (For interpretation of the references to colour in this figure legend, the reader is referred to the Web version of this article.).

Figure.5 Thermal variation of cpT for 1. The solid red line is the best fit to the proposed model. (For interpretation of the references to colour in this figure legend, the reader is referred to the Web version of this article.).

FIGURE 1

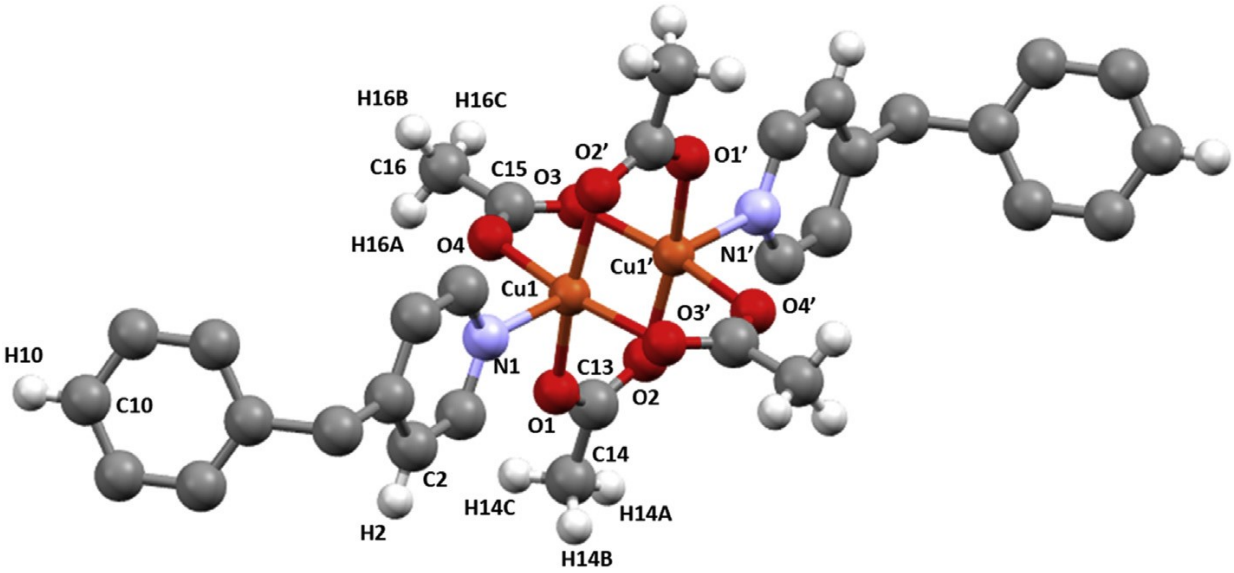
H16B
H16C
C16
C15
O3
O2'
O1'
H16A
O4
Cu1'
N1'
Cu1
O3'
O4'
H10
N1
C13
C10
O2
O1
C14
C2
H14C
H14A
H2
H14B

FIGURE 2

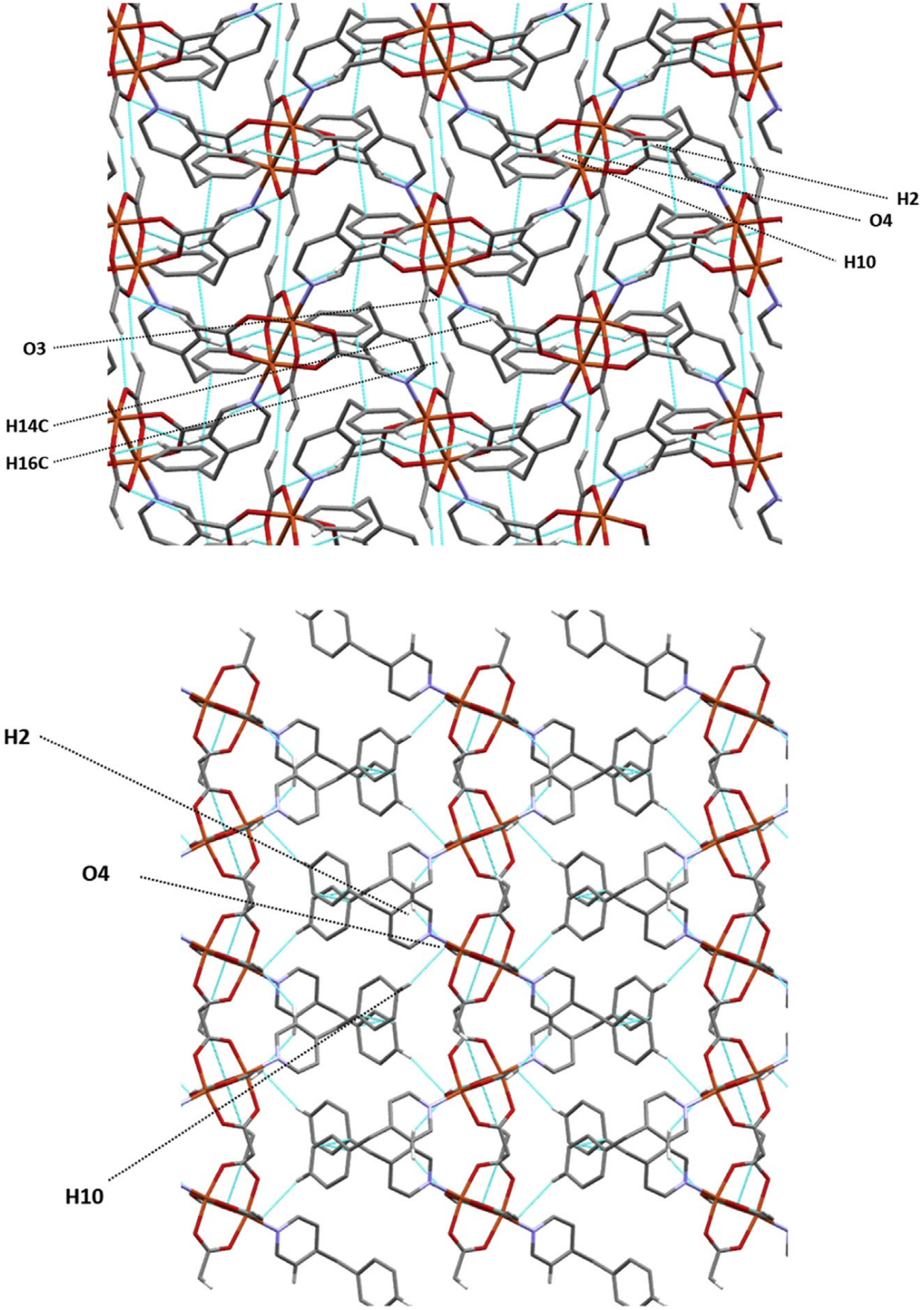

FIGURE 3

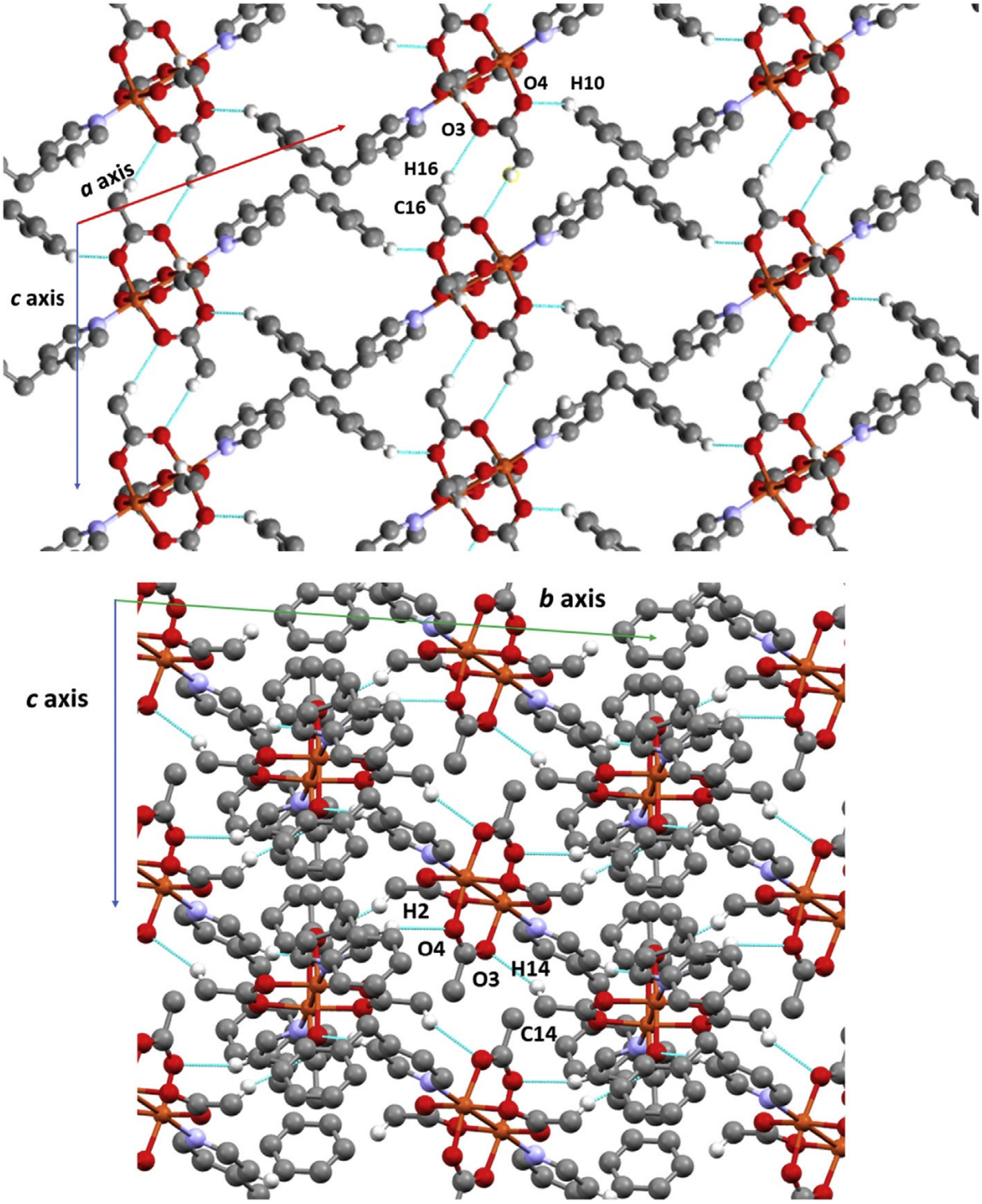

FIGURE 4

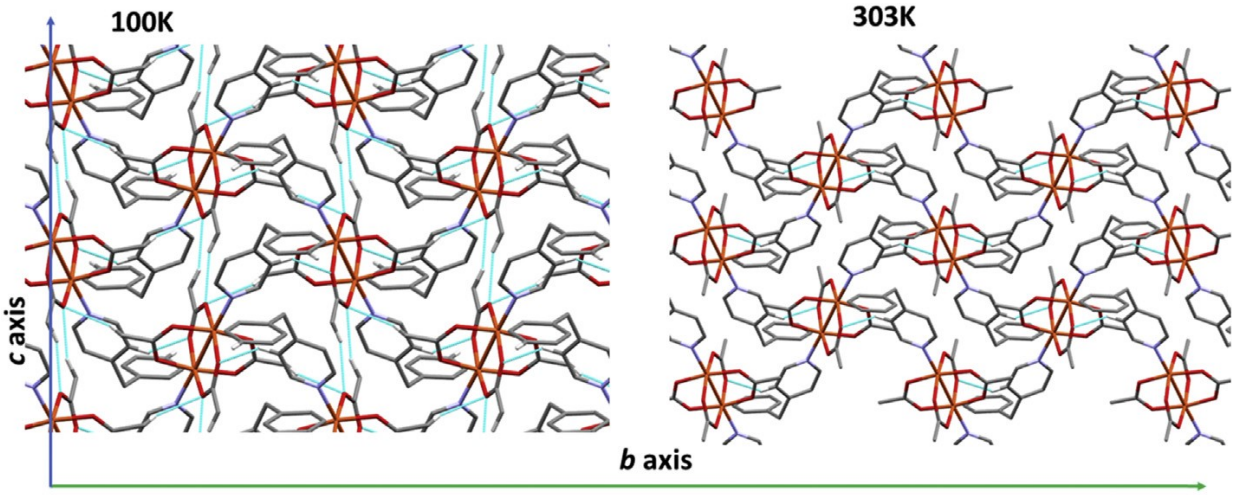

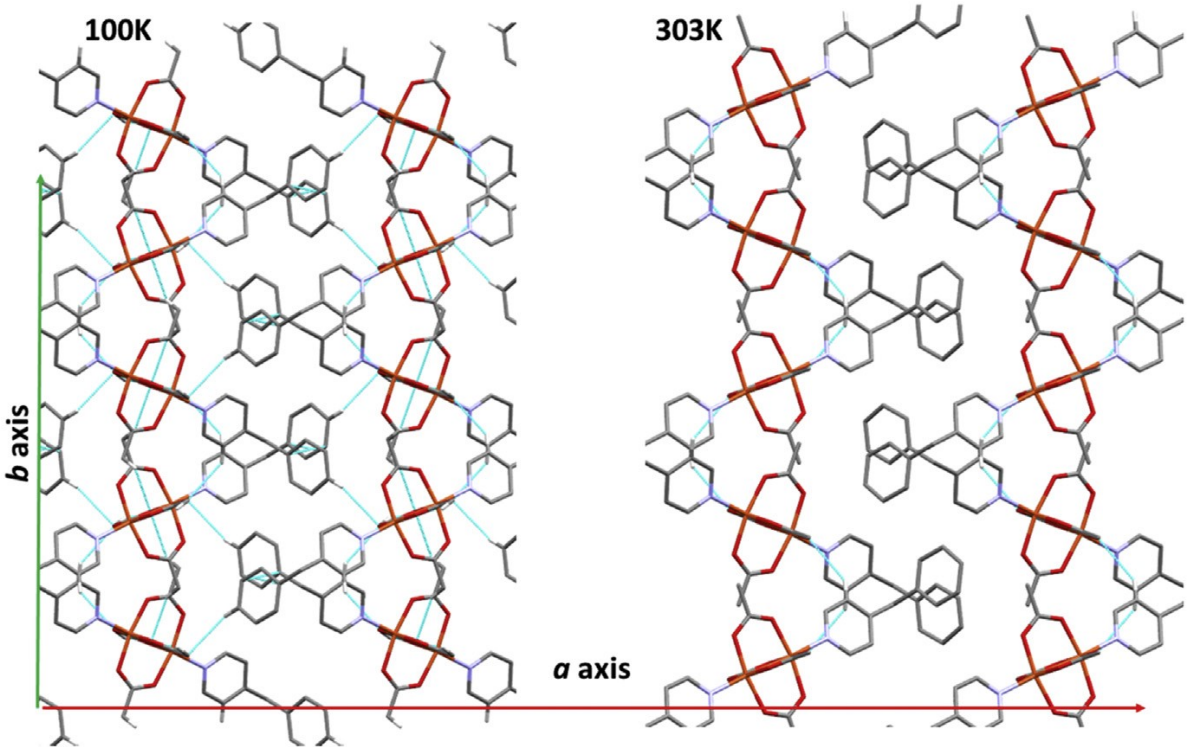

410 **FIGURE 5**

411

412

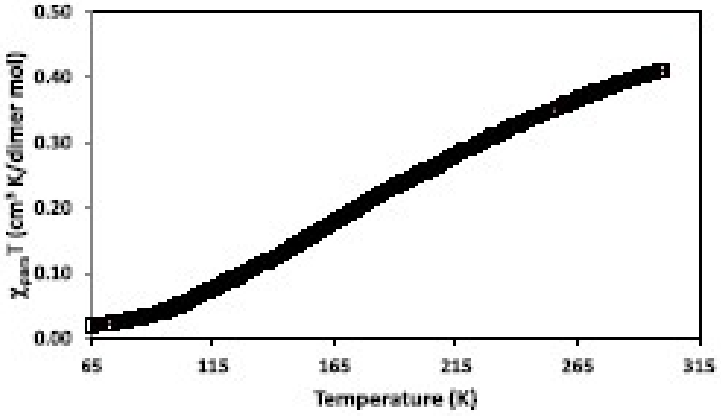

413

414

Table 1. Selected bond lengths (Å) and bond angles (°) for 1A (100 K) and 1B (303 K).

Bond length (Å)	1A (100 K)	Bond length (Å)	1B (303 K)
Cu(1)–O (1)#1	1.9637 (18)	Cu(1)–O (1)	1.975 (4)
Cu(1)–O (2)	1.9690 (18)	Cu(1)–O (2)#1	1.963 (4)
Cu(1)–O (3)	1.9695 (18)	Cu(1)–O (3)	1.962 (4)
Cu(1)–O (4)#1	1.9715 (18)	Cu(1)–O (4)#1	1.973 (4)
Cu(1)–N (1)	2.1828 (19)	Cu(1)–N (1)	2.191 (4)
Cu(1)–Cu(1)#1	2.6222 (6)	Cu(1)–Cu(1)#1	2.6311 (10)
Bond Angles (°)			
O (1)#1-Cu(1)-O (2)	168.60 (7)	O (1)-Cu(1)-O (2)#1	167.81 (15)
O (1)#1-Cu(1)-O (3)	90.27 (9)	O (1)-Cu(1)-O (3)	88.52 (18)
O (2)-Cu(1)-O (3)	88.58 (8)	O (2)#1-Cu(1)-O (3)	89.67 (17)
O (1)#1-Cu(1)-O (4)#1	89.30 (8)	O (4)#1-Cu(1)-O (1)	90.26 (18)
O (2)-Cu(1)-O (4)#1	89.58 (8)	O (2)#1-Cu(1)-O (4)#1	89.04 (18)
O (3)-Cu(1)-O (4)#1	168.52 (7)	O (3)-Cu(1)-O (4)#1	168.12 (15)
O (1)#1-Cu(1)-N (1)	93.52 (7)	O (1)#1-Cu(1)-N (1)	94.62 (15)
O (2)-Cu(1)-N (1)	97.88 (7)	O (2)#1-Cu(1)-N (1)	97.57 (15)
O (3)-Cu(1)-N (1)	94.54 (7)	O (3)-Cu(1)-N (1)	98.11 (15)
O (4)#1-Cu(1)-N (1)	96.94 (7)	O (4)#1-Cu(1)-N (1)	93.77 (15)

#1 -x+1,-y+1,-z+1.

Table 2 Distances (Å) and angles (°) related to hydrogen bonding interactions for 1A (100 K) and 1B (303 K).

	C–H···O	C–H	H···C···O	C–H···O	Symmetry code
1A					
C16–H16C···O3	2.548	0.980	3.482	159.16	1-x, 1-y, z
C14–H14C···O3	2.646	0.980	3.538	151.46	1-x, ½+y, 3/2-z
C2–H2···O4	2.595	0.950	3.349	136.54	1-x, 3/2-y, ½+z
C10–H10···O4	2.775	0.950	3.603	146.27	
1B					
C16–H16C···O3	2.751	0.960	3.581	145.15	1-x, 1-y, 2-z
C14–H14C···O3	2.737	0.959	3.609	151.41	1-x, −1/2 + y, 3/2-z
C2–H2···O4	2.672	0.930	3.426	138.67	1-x, −1/2 + y, 3/2-z
C10–H10···O4	2.877	0.930	3.700	148.15	2-x, ½+y, 3/2-z

Table 3 Crystallographic data for [Cu(MeCO2)2(4-Bzpy)]2 (1) (1A 100K, 1B 303 K).

	1A (100 K)	1B (303 K)
Formula	$C_{32}H_{34}N_2O_8Cu_2$	$C_{32}H_{34}N_2O_8Cu_2$
Formula Weight	701.69	701.69
Temperature (K)	100 (2)	303 (2)
Wavelength (Å)	0.71073	0.71073
System, space group	Monoclinic, $P2_1/c$	Monoclinic, $P2_1/c$
a (Å)	14.0442 (12)	14.0888 (8)
b (Å)	13.1036 (10)	13.2921 (7)
c (Å)	8.6257 (7)	8.7292 (5)
α (°)	90	90
β (°)	106.611 (3)	106.406 (2)
γ (°)	90	90
U (Å^3)/Z	1521.1 (2)/2	1568.16 (15)/2
D_{calc} (g cm^{-3})/μ (mm^{-1})	1.532/1.453	1.486/1.409
F (000)	724	724
Crystal size (mm^3)	0.140 × 0.112 × 0.075	0.506 × 0.120 × 0.091
hkl ranges	$-17 \le h \le 17$, $-16 \le k \le 16$, $-10 \le l \le 10$	$-17 \le h \le 17$, $-16 \le k \le 16$, $-10 \le l \le 10$
2θ Range (°)	2.914 to 26.063	2.149 to 26.399
Reflections collected/ unique/[R_{int}]	16918/3013 [R (int) = 0.0581]	20586/3193 [R (int) = 0.0342]
Completeness to θ (%)	99.9	99.3
Absorption correction	Semi-empirical	Semi-empirical
Max. and min. trans.	0.7453 and 0.5924	0.7454 and 0.6490
Data/restrains/parameters	3013/0/201	3193/0/201
Goodness-of-fit on F^2	1.043	1.167
Final R indices [I > 2σ (I)]	$R_1 = 0.0324$, $wR_2 = 0.0763$	$R_1 = 0.0517$, $wR_2 = 0.1633$
R indices (all data)	$R_1 = 0.0443$, $wR_2 = 0.0812$	$R_1 = 0.0566$, $wR_2 = 0.1693$
Extinction coefficient	n/a	n/a
Largest diff. peak and hole (e Å^{-3})	+0.503, −0.441	+1.272, −0.670